

Polarized-Neutron Study of Hematite*†

R. NATHANS

Brookhaven National Laboratory, Upton, New York

S. J. PICKART AND H. A. ALPERIN

*U. S. Naval Ordnance Laboratory, Silver Spring, Maryland and
Brookhaven National Laboratory, Upton, New York*

P. J. BROWN‡

Brookhaven National Laboratory, Upton, New York

(Received 7 July 1964)

Polarized-neutron studies on natural and synthetic single crystals of hematite have shown that the 180° antiferromagnetic domain walls are removed in low fields as the parasitic ferromagnetism of the high-temperature phase is saturated, and the remaining 120° walls are removed by the application of higher fields. No memory effect was observed for the antiferromagnetic domain configuration as the crystal was cycled through the spin-axis transition temperature. The spin density of the ferromagnetic component of the spin system was found to be different from that of the antiferromagnetic component.

I. INTRODUCTION

HEMATITE ($\alpha\text{-Fe}_2\text{O}_3$) has been the subject of numerous investigations aimed at determining the relation of its weak spontaneous moment to its primarily antiferromagnetic structure. The present work represents an attempt to gain further information about this situation by the use of polarized neutron scattering.

Magnetic measurements by Smith,¹ Néel and Pauthenet,² Lin,³ Tasaki and Iida,⁴ and others,⁵ have established that there exists, above 260°K , a spontaneous moment of approximately 0.36 emu/gm, confined to the basal plane; various other experiments by Tasaki *et al.*⁶ demonstrated that this moment is not due to impurities or to differing oxidation states of the iron, and is presumably therefore an intrinsic property. The powder neutron diffraction studies of Shull *et al.*,⁷ led to the basic antiferromagnetic structure, which is illustrated for the hexagonal unit cell in Fig. 1. It consists of the spins within each "puckered" hexagonal plane of Fe atoms being coupled parallel, while alternating planes are arranged antiparallel. This work also showed that the spin direction changed from within the basal plane above the 260°K transition to along the trigonal axis below it.

The most recent explanation of these phenomena was put forward by Dzyaloshinskii⁸ on the basis of the magnetic symmetry of the hematite structure and the Landau theory of phase transitions. According to his arguments, in the high-temperature phase the spins are slightly canted toward each other from one plane to the next, giving rise to a small net moment confined to the plane. This situation arises because the symmetry allows a term in the free energy of the form $\mathbf{D} \cdot (\mathbf{S}_i \times \mathbf{S}_j)$, where \mathbf{D} is along the trigonal axis and i and j are all pairs of atoms not related by a center of symmetry. The origin of this term was later ascribed by Moriya⁹ to the anisotropic superexchange interaction. He showed that the coefficient of the Dzyaloshinskii term was of the order of $(\Delta g/g)J$, where J is the isotropic exchange interaction, and thus was able to explain the smallness of the effect for $\alpha\text{-Fe}_2\text{O}_3$.

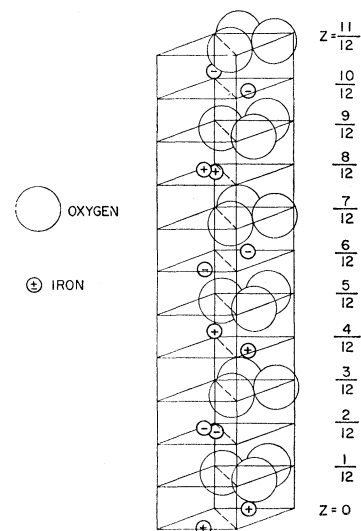


FIG. 1. The unit cell of hematite (not to scale) showing the crystal and magnetic structure. The hexagonal unit cell is used in order to show more clearly the planes of Fe atoms with parallel spin, and the differing oxygen coordination for Fe atoms with opposite spin. The Fe atoms are shifted up and down from the planes (whose z coordinate is given at the right) by an amount $\pm 0.022c$.

* Work performed under the auspices of the U. S. Atomic Energy Commission.

† Previously reported briefly in *J. Appl. Phys.* **34**, 1200 (1963), and in *J. Phys. Radium* **25**, 542 (1964).

‡ Present address: Cavendish Laboratory, Cambridge, England.

¹ T. T. Smith, *Phys. Rev.* **8**, 721 (1916).

² L. Néel and R. Pauthenet, *Compt. Rend.* **234**, 2172 (1952); *L. Néel, Rev. Mod. Phys.* **25**, 58 (1953).

³ S. T. Lin, *Phys. Rev.* **116**, 1447 (1959); *J. Phys. Soc. Japan* **17**, Suppl. B-I, 226 (1962).

⁴ A. Tasaki and S. Iida, *J. Phys. Soc. Japan* **18**, 1148 (1963).

⁵ R. Chevallier, *J. Phys. Radium* **12**, 172 (1951); F. J. Morin, *Phys. Rev.* **78**, 819 (1950); C. Gillaud, *J. Phys. Radium* **12**, 489 (1951).

⁶ A. Tasaki, K. Siratori, and S. Iida, *J. Phys. Soc. Japan* **15**, 1535 (1960); A. Tasaki and S. Iida, *ibid.* **16**, 1697 (1961).

⁷ C. G. Shull, W. A. Strauser, and E. O. Wollan, *Phys. Rev.* **83**, 333 (1951).

⁸ I. Dzyaloshinskii, *Phys. Chem. Solids* **4**, 241 (1958).

⁹ T. Moriya, *Phys. Rev.* **120**, 91 (1960).

There are two reasons for the application of the polarized neutron technique to this problem. First, we can observe the effects of applied magnetic fields on the antiferromagnetic domain distribution, thereby relating the behavior of the antiferromagnetic lattice to the ferromagnetic moment. This information is of use in establishing the nature of the magnetization process in this and other canted antiferromagnetic structures. Furthermore, we can measure the spin density distribution of the ferromagnetic moment, which is relevant in discussing the nature of the Dyzalooshinskii mechanism in these magnetic structures.

II. POLARIZED NEUTRON SCATTERING FROM ANTIFERROMAGNETIC CRYSTALS

Hematite, like MnF_2 , satisfies the conditions for a polarization dependence of the antiferromagnetic scattering.¹⁰ Basically, this arises because the cations forming the antiparallel sublattices are not related by a simple translation. The different orientation of the distorted anion octahedra coordinating two antiparallel spins (such as those at $z=4/12$ and $6/12$ in Fig. 1) contributes nuclear scattering to the antiferromagnetic reflections, with which the magnetic scattering can interfere constructively or destructively, depending on the sign of the cation spin relative to that of the incident neutron spin state. This effect appears in a measurement of the polarization ratio, defined as the ratio of intensities for incoming neutrons parallel or antiparallel to a given direction:

$$R = \frac{F_N^2 + F_M^2 q^2 + 2\beta F_N F_M \mathbf{q} \cdot \boldsymbol{\lambda}}{F_N^2 + F_M^2 q^2 - 2\beta F_N F_M \mathbf{q} \cdot \boldsymbol{\lambda}}, \quad (1)$$

where F_N is the nuclear and F_M the magnetic structure factor, $\mathbf{q} = \boldsymbol{\varepsilon}(\boldsymbol{\varepsilon} \cdot \mathbf{K}) - \mathbf{K}$ ($\boldsymbol{\varepsilon}$ is the scattering vector, \mathbf{K} the ion spin unit vector), $\boldsymbol{\lambda}$ is the neutron polarization direction, and β is a parameter related to the antiferromagnetic domain configuration. The amount of interference will obviously be lessened if some fraction of the spins on equivalent sites is reversed; this fraction is given by $(1+\beta)/2$. If there is an equal proportion of up and down domains, $\beta=0$, and the polarization dependence disappears. Thus, this dependence can be used to determine the population of 180° antiferromagnetic domains, provided that $\boldsymbol{\lambda} \cdot \mathbf{q} \neq 0$ (which in our arrangement means that the spins have components along the polarization direction) and the structure factors are known. Conversely, if the domain distribution has been determined, the polarization ratio can be used to determine the magnetic form factor, which enters the magnetic structure factor F_M .

The analysis of the polarization ratios in terms of the domain apportionment in hematite is more complicated than in the uniaxial MnF_2 . In hematite at room tem-

perature there are three equivalent antiferromagnetic axes in the basal plane along which the magnetic spins may lie. We shall henceforth refer to these as trigonal domains, since they are related by a spin axis rotation of 120° . Since within each of these trigonal domains there can exist 180° domains, Eq. (1) must be modified to take account of the variation in the value of β and \mathbf{q} from one trigonal domain to another. The expression becomes simply

$$R = \frac{F_N^2 + F_M^2 (q^2)_{\text{av}} + 2F_N F_M (\beta \mathbf{q} \cdot \boldsymbol{\lambda})_{\text{av}}}{F_N^2 + F_M^2 (q^2)_{\text{av}} - 2F_N F_M (\beta \mathbf{q} \cdot \boldsymbol{\lambda})_{\text{av}}}, \quad (2)$$

where the average is taken over the trigonal domains.

We can obtain information on the distribution of these trigonal domains by an analysis of the final polarization of the scattered neutrons. The final polarization of an elastically scattered beam¹¹ for the case of a purely magnetic reflection can be written

$$\mathbf{P}_f = 2\hat{q}(\hat{q} \cdot \mathbf{P}_i) - \mathbf{P}_i,$$

where \hat{q} is a unit vector along \mathbf{q} . In the present arrangement, the polarization is analyzed along the initial polarization direction $\boldsymbol{\lambda}$, giving, for complete initial polarization ($|\mathbf{P}_i|=1$)

$$\boldsymbol{\lambda} \cdot \mathbf{P}_f = P_f = 2 \cos^2 \theta - 1, \quad (3)$$

where θ is the angle between $\boldsymbol{\lambda}$ and \mathbf{q} . Since the neutrons in the present instance are polarized \perp to $\boldsymbol{\varepsilon}(\boldsymbol{\lambda} \cdot \mathbf{q} = -\boldsymbol{\lambda} \cdot \mathbf{K})$, the expression (3) shows that unless there are spin components \perp to $\boldsymbol{\lambda}$, no polarization change will occur. Consequently, the fraction that are flipped can be related to the perpendicular component of the spins in each of the trigonal antiferromagnetic domains.

Finally, by a measurement of the polarization ratio in the Bragg reflections which are forbidden by the antiferromagnetic structure, but contain contributions from the ferromagnetic component, we can evaluate the distribution within the unit cell of the ferromagnetic spin density. Referring to Eq. (1) we use the experimentally determined values of R to evaluate F_M , with \mathbf{q} , $\boldsymbol{\lambda}$, F_N , and β being known from the experimental arrangements.

III. EXPERIMENTAL RESULTS

The results to be described will be grouped under two headings, pertaining to determination of the antiferromagnetic domain wall behavior, and to measurements of the magnetic form factor or spin-density distribution of the ferromagnetic component of the spin system.

A. Antiferromagnetic Domains in $\alpha\text{-Fe}_2\text{O}_3$

In a canted antiferromagnet, one can visualize 180° ferromagnetic domain walls (FW), in which the ferromagnetic component changes direction, and antiferro-

¹⁰ H. A. Alperin, P. J. Brown, R. Nathans, and S. J. Pickart, Phys. Rev. Letters **7**, 237 (1962).

¹¹ M. Blume, Phys. Rev. **130**, 1670 (1963).

magnetic walls (AFW), in which the antiferromagnetic component reverses. The situation is illustrated in Fig. 2, where case (a) schematically represents a single domain crystal and (b)–(d) represent the other possibilities: FW alone, AFW alone, or FW and AFW in coincidence. It will be noted that only in the last case is the sense of \mathbf{D} in the Dzyaloshinskii term invariant throughout the crystal; hence one would expect for a perfect crystal that if FW's and AFW's exist, they must be coupled together. From this coupling it would follow that the field dependence of the magnetization should be reflected in the field dependence of the AFW population, that is, it should not be possible to saturate the ferromagnetic moment without making an essentially single antiferromagnetic domain of the crystal. For any other model of the origin of the parasitic ferromagnetism, however, this coincidence will not necessarily occur.

The first of the measurements to be reported which bear on this question is the field dependence of the polarization ratio for the rhombohedral (210) reflection. (In what follows we use Miller indices and zone axes referred to the rhombohedral cell). This is a reasonably intense reflection and possesses nuclear and magnetic structure factors (F_N and F_M) which are approximately equal, thus insuring a strong sensitivity to β or the degree of single domainness. In the course of these observations, measurements were made for a number of crystallographic orientations with respect to the applied field, and on both natural and synthetic crystals. Typical results of these measurements are shown in Fig. 3 together with a magnetization curve for hematite. In every case a peak in the polarization ratio reproducible in its gross features occurred at relatively low fields, the highest ratio usually being around 1.3–1.4 although values as high as 2.0 were observed on occasion. We also found a hysteresis effect in the

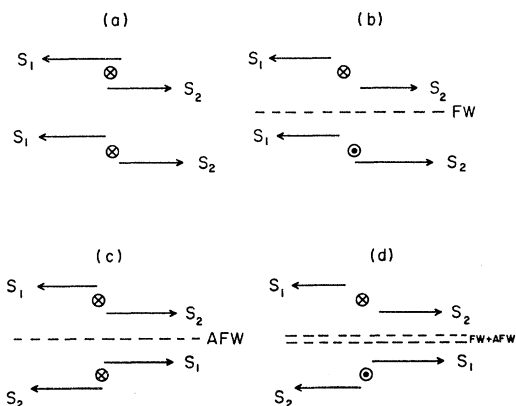


FIG. 2. Schematic representation of possible domain wall configurations in the high-temperature phase of hematite. The S_1 's and S_2 's represent equivalent neighboring spins in different regions of the crystal. The c axis is vertical and in the plane of the paper, so that the symbols \otimes and \odot represent the cant (and the ferromagnetic component) into and out of the plane of the paper, respectively.

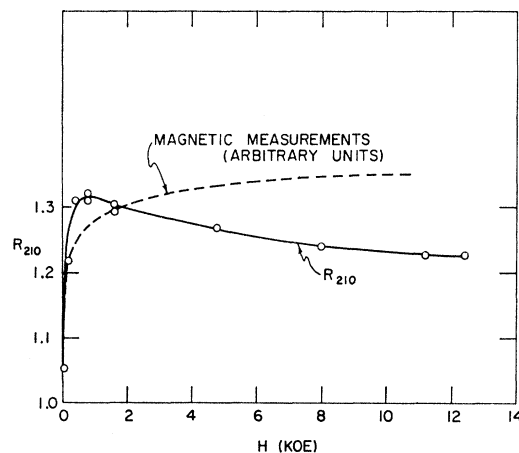


FIG. 3. Polarization ratio of the (210) reflection as a function of applied field at room temperature. These data were taken on a natural crystal with the $[111]$ axis tilted 28.6° from the field direction, so that the component of the field in the (111) plane is $\sim \frac{1}{2}$ the applied field.

polarization ratio, indicating that the crystals did not return to their virgin state of a random AFW distribution when the field was removed. This increase in the polarization dependence of the neutron scattering establishes that there is a decrease in the number of 180° AFW's at low magnetic fields where the ferromagnetism begins to saturate.

While the sharp rise observed in the polarization ratio shown in Fig. 3 is thus easily accounted for, the subsequent decrease requires further consideration. The explanation for this behavior is to be found in the field dependence of the trigonal domain population. To determine this variation with field, the neutron beam was reflected from the purely magnetic (111) Bragg reflection onto a third crystal, which analyzed the state of polarization in the final beam. The final polarization of the (111) reflected beam from a natural crystal is shown in Fig. 4, for two different orientations of the crystal with respect to the field direction. The polarization starts from zero at zero field and attains a value of -1 in high fields, a result confirming and extending previous unpublished results of Nathans *et al.*¹² The value of -1 observed for P_f in high fields means according to (3) that $\langle \cos^2\theta \rangle_{av} = 0$ and the spins are all perpendicular to the field. The zero polarization in zero fields (which was checked and found not to be due to transmission) can of course arise in many ways, but a model which gives the observed isotropic dependence on the azimuth angle of the plane and also satisfies the crystal symmetry is a random distribution of the trigonal domains.¹³

¹² R. Nathans, T. Riste, G. Shirane, and C. G. Shull, M. I. T. Structure of Solids Group, Technical Report No. 4, 1958 (unpublished).

¹³ It should be noted that, with such a domain distribution, it is impossible to specify the spin direction within the basal plane from unpolarized-neutron measurements.

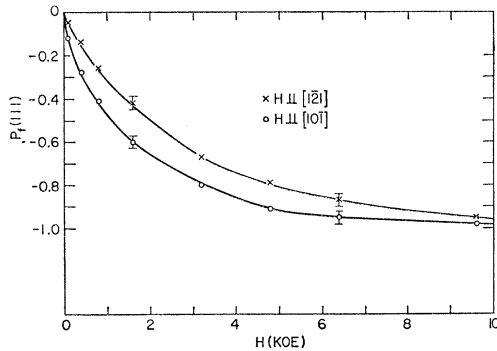


FIG. 4. Final polarization of the (111) reflected beam from a natural crystal as a function of field, applied in two directions within the (111) plane. A synthetic crystal showed similar behavior but saturated in somewhat lower fields.

With these results on the trigonal domain distribution, we can now return to a more quantitative analysis of the polarization ratio measurements on the (210) reflection, which according to Eq. (2) should represent an average taken over the trigonal domains, each with its appropriate 180° domain parameter ($-1 < \beta < 1$). Using the appropriate values of F_M and F_N for the (210) reflection, we can relate the observations to antiferromagnetic domain behavior in terms of the following simple model. With the assumption of an isotropic population of trigonal domains in low fields, the maximum R_{210} obtainable is 2.2 if the easy direction is taken as $[10\bar{1}]$ or 1.4 if $[\bar{1}\bar{2}1]$ (the direction of the twofold axis and glide plane, respectively). These values are obtained by setting $|\beta_i| = 1$ ($i = 1, 2, 3$) and assigning the direction (i.e., relative phases of trigonal domains) in the most favorable way. Since the maximum observed polarization ratios lay in this range, we may conclude that in the low fields we have very nearly 180° domains within each trigonal domain. This conclusion is reinforced by the fact that the model correctly predicts the measured final polarization of the (210) reflected beam.

Combining this result with the final polarization data described in the previous paragraph seems to indicate that the action of the field is first to sweep out antiferromagnetic walls within each trigonal domain, and then to gradually repopulate these domains so as to make the spins more perpendicular to the field. It is this repopulation of the trigonal domains that accounts for the drop in R_{210} from its peak value. As the spin in each trigonal domain becomes more perpendicular to the applied field, $\lambda \cdot \mathbf{q} \rightarrow 0$ and hence $R_{210} \rightarrow 1$; since at the same time the ferromagnetic component is being aligned, we have established a correlation between the motion of the ferromagnetic and antiferromagnetic walls. It follows that these walls must coexist in the unmagnetized state as required by the Dzyaloshinskii model.

If this picture is correct, it should also be possible to relate these neutron data to the observed magnetization curve of the ferromagnetic component. This can be done

only with some ambiguity, however, since the neutron measurements on final polarization give $\langle \cos^2\theta \rangle_{av}$, where θ is the angle between H and the antiferromagnetic component, and the magnetization measures $\sim \langle \sin\theta \rangle_{av}$. Nevertheless, in Fig. 5 we plot magnetization curves constructed from the two curves in Fig. 4, compared to a scaled 300°K isotherm as measured by Lin³ (less the susceptibility term, to which the final polarization data are insensitive). The approach to saturation as measured by neutrons is seen to be not inconsistent with the magnetization data.

In the course of these experiments, we also investigated the (210) polarization ratio below the magnetic transition at 260°K , where the spins are directed along the c axis.¹⁴ We found that it was necessary to cool the crystal in a magnetic field of several hundred oersteds to obtain a high polarization ratio below the transition; furthermore, the effects of such annealing fields were most pronounced when applied along the c axis. It thus appears that the more single domain above the transition the crystal is, the more likely it is to remain single after the spins have rotated through 90° from the basal plane, suggesting that the spins' rotation is more a cooperative than a statistical phenomenon. When the crystal was cycled through the transition in the weak field necessary to maintain the neutron polarization (~ 20 G), no correlation was found with the initial antiferromagnetic domain configuration. This is consistent with the recent observation by Tasaki and Iida⁴ that there is no memory effect of the remanent moment

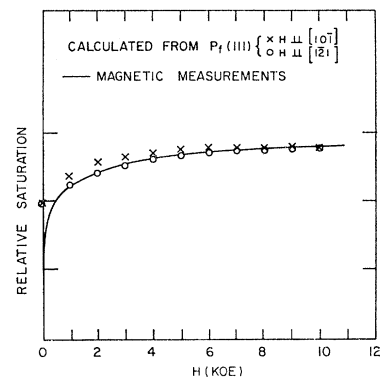


FIG. 5. Relative saturation of the ferromagnetic component as calculated from the curves of Fig. 4, compared with magnetic measurements. We assume a single 180° domain within each 120° domain, which is probably the case for all points above zero field.

¹⁴ Recently Morrish, Johnston, and Curry [Phys. Letters 7, 177 (1963)] have measured a residual (111) intensity below the transition, which they attribute to a 10° tilt of the spins away from the c axis. We repeated these measurements, rotating around the scattering vector to check for the presence of double Bragg scattering. An angular variation of about a factor of 2 was found, but the lowest residual intensity noted was 0.8%, corresponding to a tilt angle of $\sim 5^\circ$ (neglecting possible extinction). However, it should be pointed out that this residual intensity could equally well arise from regions in the crystal (only 1% by volume) where, perhaps due to impurities or imperfections, the local anisotropy constant K_1 does not change sign.

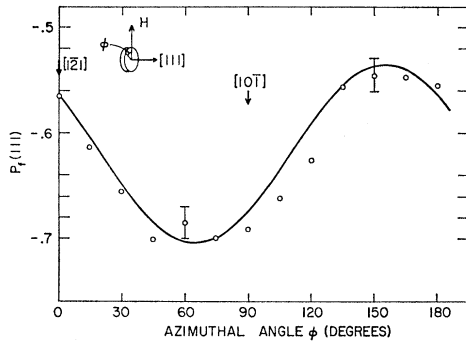


FIG. 6. Final polarization of the (111) beam reflected from a disk-shaped natural crystal oriented as shown in a constant field of 2400 Oe. The solid line is a $\sin 2\phi$ curve fitted at $\phi=0$.

in a single crystal, bearing in mind the coincidence of walls mentioned above.

There are two other aspects of the observations that are not understood at the present time but should nevertheless be mentioned. First is the slight difference observed in the final polarization in Fig. 3 when the crystal was oriented with the field in different directions in the (111) plane. This effect was investigated more thoroughly in a natural crystal by cutting a crystal in the shape of a disk with a (111) face. With this shape as the crystal is rotated around [111] no changes are introduced by extinction or depolarization. The final polarization observed upon rotation, as plotted in Fig. 6, shows an apparent 180° symmetry. Evidence for a twofold symmetry is also to be found in the torque curves obtained by Tasaki and Iida.⁴ Since the torque curves are principally determined by the ferromagnetic component, while the neutron observations assess the behavior of the antiferromagnetic lattice, we are led again to the correlation between the ferromagnetic moment and the antiferromagnetic lattice. Although the origin of the uniaxial symmetry is presumably the same in the two cases, there is no good explanation for it at present.

Another puzzling phenomenon we observed was a nonequivalence of R_{210} and $R_{\bar{2}\bar{1}0}$, either when the crystal was rotated around the field direction (which is the axis of the spectrometer) or viewed from the antiparallel setting. Normally this sort of behavior might be ascribed to severe extinction plus a different domain type existing on different sides of the crystal, but various experiments employing cadmium masking and crystals of various sizes and shapes indicated that this was unlikely. It is even more unlikely in view of the fact that the peak observed value of R_{210} is almost as large as allowed by the antiferromagnetic domain structure; extinction severe enough to prevent the beam from penetrating the whole crystal would certainly lower the larger intensity in (2) considerably. Moreover, this effect disappeared: (a) when the crystal was rotated around the (210) scattering vector to a position in which the (111) plane was vertical; (b)

when the temperature was lowered below the 260°K transition. In the great majority of cases, the relation was reciprocal, i.e., $R_{210}=1/R_{\bar{2}\bar{1}0}$, which according to (2), indicates a change in sign of the interference term. This could certainly occur if the nuclear structure factor F_N changes sign; such cannot be the case if the space group of hematite is $R\bar{3}c$. The remaining possibility is that the antiferromagnetic component of the spin system changes sign, although the origin of the mechanism for such a rotation is obscure.¹⁵ The experiments cited definitely connect this effect with the parasitic ferromagnetism; further experiments on field cooling through the Néel point introduced some permanent changes in a particular crystal, destroying the reciprocity but not the nonequivalence; these facts taken together suggest domain wall effects, but no satisfactory explanation has been forthcoming.

B. Spin Density of the Canted Moment

The antiferromagnetic structure of hematite shown in Fig. 1 gives rise to reflections with $(h+k+l)$ odd; if the spins are canted in the way predicted by Dzyaloshinskii, there is also a magnetic contribution to the reflections with $(h+k+l)$ even, proportional to the magnitude of the ferromagnetic component. Although this moment amounts to only about $0.005 \mu_B/\text{iron atom}$, it is within the limits of observation for several favorable cases. In order to verify the existence of the canted moment and determine its spin density distribution, it was decided to measure the polarization ratio of these reflections.

In practice, the number of reflections available for this study is severely restricted by several factors. First, to make the effect observable the ratio F_M/F_N must be larger than $\sim 10^{-3}$; this means F_N must be small, limiting us to reflections where the iron and oxygen structure factors are out of phase. Secondly, there is a contribution to these same reflections from the antiferromagnetic spins if there is covalent spin density¹⁶ in the iron-oxygen bonds; this contamination is avoided if one measures only reflections belonging to zones lying within the (111) plane, since then in fields sufficient to turn the antiferromagnetic spin system perpendicular, the interference term [proportional to $\lambda \cdot \mathbf{q}$ in (1)] is zero. (The $F_M^2 q^2$ term which remains is negligible with respect to F_N^2 .) A further simplification results for the ferromagnetic component upon saturation since $\lambda \cdot \mathbf{q}$ is always ± 1 and $q^2=1$.

As a result of these restrictions, only four reflections could be feasibly measured: (222), (002), (114), and (330). The latter pair are equivalent in the hematite

¹⁵ The possibility of a small transverse component of the field (fixed in space) flipping the antiferromagnetic component, through the coupling with the ferromagnetic moment, was ruled out by experiment.

¹⁶ R. Nathans, H. A. Alperin, S. J. Pickart, and P. J. Brown, J. Appl. Phys. **34**, 1182 (1963).

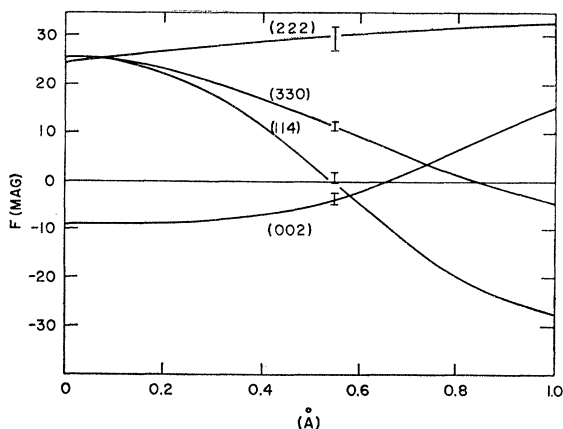


FIG. 7. Calculated magnetic structure factors for $(h+k+l)$ even (arbitrary units) for the isolated spherical charge model plotted as a function of the displacement of the charge from the Fe position. The values measured on a synthetic crystal are plotted as vertical bars.

structure, i.e., they have the same structure factor and Bragg angle. In the calculation of the expected R_{210} in the previous section, we assumed in obtaining F_M the form factor¹⁷ for Fe^{3+} , which was found to satisfy the magnetic intensities in a powdered Fe_2O_3 sample.¹⁸ In calculating the expected magnitude of R for the above reflections we at first used the same form factor. The actual observations, which were checked for double Bragg scattering and assumed to be extinction-free because of their extremely low scattering power, differed considerably from these estimates, as can be seen from Table I.

Since the magnetic scattering is scaled by the nuclear [Eq. (1) is solved for the ratio F_M/F_N], these results depend on the structural parameters, especially since they arise from difference peaks. In the present calculations we used parameters derived from a very recent single crystal x-ray refinement by Zoltai.¹⁹ However, as mentioned above, the pair (114, 330) must be equal, irrespective of the value of the atomic parameters; the difference observed in Table I necessarily leads to the conclusion that the ferromagnetic spin density cannot be symmetrically located on the iron atom positions,

TABLE I. Comparison of calculated and observed magnetic structure factors.

hkl	$(\sin\theta)/\lambda$	F_M/F_N	F_{Mobs} (10^{-14} cm)	F_{Mcalc} (10^{-14} cm)
(002)	0.240	$+0.0010 \pm 0.0004$	-0.011 ± 0.004	-0.070
(222)	0.217	-0.0025 ± 0.0002	$+0.213 \pm 0.020$	+0.216
(114)	} 0.407 {	-0.0003 ± 0.0005	$+0.005 \pm 0.008$	+0.079
(330)		-0.0045 ± 0.0004	$+0.082 \pm 0.007$	+0.079

¹⁷ R. Nathans, S. J. Pickart, and H. A. Alperin, J. Phys. Soc. Japan 17, Suppl. B-III, 7 (1962).

¹⁸ D. E. Cox, W. J. Takei, R. C. Miller, and G. Shirane, Phys. Chem. Solids 23, 863 (1962).

¹⁹ T. Zoltai, A. C. A. Cambridge Meeting, 1963 (unpublished).

but must be placed at least partly on the general position in $R\bar{3}c$.²⁰

A first attempt was made to explain these observations by using an isolated center-of-magnetic-charge model such as adopted¹⁴ in MnF_2 . It soon became clear, however, that the nonequivalence of (114, 330) placed rather severe restrictions on the possible location of such charge; for instance, it cannot be placed along the iron-oxygen bond directions or be symmetrically disposed about these directions. However, the next obvious choice, namely, retaining the symmetry of the near-neighbor iron atoms within each plane, leads to excellent agreement. The magnetic structure factors, on the same scale (not absolute), are graphed in Fig. 7 as a function of the charge displacement from the iron site. It is apparent that a solution exists in the neighborhood of $y=0.5$, where (222) is large and positive, (002) small and negative, and at the same time (330) is large and positive while (114) is small. To obtain the fit shown, we made the further reasonable assumption that the ferromagnetic charge is confined to a sphere of radius ≈ 0.2 Å.

This model, although predicting the observed structure factors, is admittedly oversimplified and can indicate only gross features of the ferromagnetic spin density. Recently, Kaplan²¹ has performed a theoretical calculation of the spin density based upon the magnetic symmetry of the hematite lattice which also predicts a splitting of (114, 330). Furthermore, the calculation predicts a nonzero contribution for these two peaks below the transition, of the same order of magnitude as above. An attempt made to observe this during the low-temperature measurements was unsuccessful because of the failure to obtain a sufficiently large single antiferromagnetic domain population.

IV. DISCUSSION AND CONCLUSIONS

The polarized-neutron measurements described here lend considerable support to the Dzyaloshinskii-Moriya model of "canted" antiferromagnetism as responsible for the weak ferromagnetism in hematite, primarily because of the intimate connection between the changes in the antiferromagnetic domain structure and the increase in the aligned ferromagnetic component. A consequence of this interrelationship is the expectation of relatively sizable remanent moments and coercive forces in canted arrangements where the anisotropy is large. This follows from the necessity to reform antiferromagnetic domain walls upon demag-

²⁰ We refer here to the "nonmagnetic" space group-symmetry: strictly considered, the symmetry is lower, since with the spins in the basal plane the threefold axis is destroyed. It might be argued that slight shifts in the atomic parameters allowed by the lower symmetry, undetected in x-ray measurements of a multidomain (pseudorhombohedral) crystal, could give rise to the observed difference in (114, 330). That such shifts have actually not taken place is evidenced by the fact that we observe equal total intensities ($\cong F_N^2$) for the pair in our single domain crystal.

²¹ T. A. Kaplan, preceding article, Phys. Rev. 136, A1636 (1964).

netization, thus working against the antiferromagnetic exchange as well as the anisotropy forces.

With regard to the distribution of the ferromagnetic spin density, it is difficult on the basis of these few reflections to assign any unique interpretation to our results. What is clear, however, is that the ferromagnetic component has a significant different spin density distribution from the antiferromagnetic component. In other words, the spin density in this compound must be thought of as a vector rather than a scalar function, that is, varying spatially in direction as well as magnitude. It may very well be that this is a special case of a more general phenomenon that occurs whenever spin-orbit coupling is present. Because of the smallness of

the effect, it is impossible in the present case to get much of a detailed picture of such a spin density, other than to show that it exists and probably resides in directions away from the antiferromagnetic superexchange bonds. It is planned to investigate the phenomenon further in other antiferromagnets where the canting angle is larger, such as the rare-earth orthoferrites.

ACKNOWLEDGMENTS

We are greatly indebted to very many of our colleagues for helpful discussion of the above results, particularly Dr. M. Blume, Dr. G. Shirane, and Dr. T. Kaplan.

PHYSICAL REVIEW

VOLUME 136, NUMBER 6A

14 DECEMBER 1964

One-Dimensional Equation for a Two-Dimensional Bloch Electron in a Magnetic Field

J. ZAK*

National Magnet Laboratory,† Massachusetts Institute of Technology, Cambridge, Massachusetts

(Received 24 July 1964)

The properties of the symmetry-adapted functions for the irreducible representations of the magnetic translation group are used to derive a one-dimensional difference-differential equation for a two-dimensional Bloch electron in a constant magnetic field.

THE dynamics of an electron in a two-dimensional periodic potential and a constant magnetic field perpendicular to the plane of motion is discussed. Using symmetry-adapted functions, defined previously, an exact one-dimensional Schrödinger equation for this “two-dimensional Bloch electron in a magnetic field” has been derived. Since no approximations were introduced in this derivation, our one-dimensional equation contains all the information for describing the dynamics of the problem. By contrast, in all other existing methods, such as the effective-mass approximation, the equations are approximate.

It is well known that the energy spectrum of a free electron in a magnetic field consists of two parts: one part is connected with the motion in the direction of the magnetic field and is continuous; the other part comes from the motion in the plane perpendicular to the magnetic field and is discrete. The effective-mass approximation¹⁻³ shows that one may expect this same division of the energy spectrum to hold also in the case of a Bloch electron in a magnetic field. Since quantum

effects in solids are connected with the discrete part of the energy spectrum, it is of great interest to investigate the behavior of a Bloch electron in the plane perpendicular to the external magnetic field.

To derive the one-dimensional equation, symmetry-adapted functions for a Bloch electron in a magnetic field⁴ are used. In the case of “rational” magnetic fields^{5,6} these functions are given by

$$\psi_j^{lk}(\mathbf{r}) = \exp\{i\mathbf{k}\cdot\mathbf{r}\} \exp\left\{-i\left(j + \frac{1}{4\pi}\mathbf{K}_2\cdot\mathbf{r}\right)\frac{n}{N}\mathbf{K}_1\cdot\mathbf{r}\right\} \times w_{lk}(\mathbf{r} + j\mathbf{a}_2) \cdots \quad (1)$$

Here j takes values from 0 to $N-1$, l is the magnetic-band index, \mathbf{K}_1 and \mathbf{K}_2 are unit-cell vectors of the reciprocal lattice,

$$\mathbf{k} = m_1\mathbf{K}_1/N + m_2\mathbf{K}_2/N, \quad 0 \leq m, m_2 < 1 \quad (2)$$

⁴ J. Zak, Phys. Rev. **134**, A1602, A1607 (1964).

⁵ The rationality of the magnetic field is defined here by the relation $\mathbf{H}\cdot\mathbf{a}_1\times\mathbf{a}_2/(hc/|e|) = n/N$, where \mathbf{H} is the magnetic field, $\mathbf{a}_1, \mathbf{a}_2$ are the unit cell vectors, $hc/|e|$ is the elementary fluxon, and n, N are integers. This relation differs by a factor of 2 from the relation (42) in Ref. 4 and is more convenient, because it leads to representations of dimensionality N for both even and odd N . [See also E. Brown, Phys. Rev. **133**, A1038 (1964) and Ref. 6.]

⁶ J. Zak, Phys. Rev. **136**, A776 (1964).

* Present Address: Department of Physics, Technion-Israel Institute of Technology, Haifa, Israel.

† Supported by the U. S. Air Force Office of Scientific Research.

¹ E. I. Blount, Phys. Rev. **126**, 1636 (1962).

² A. B. Pippard, Proc. Roy. Soc. (London) **A270**, 1 (1962).

³ J. M. Luttinger and W. Kohn, Phys. Rev. **97**, 869 (1955).